Special Collection

Photophysical and Electrochemical Properties of Pyrimidopteridine-Based Organic Photoredox Catalysts

Tobias Taeufer[+],[a] Miguel A. Argüello Cordero[+],[b] Andranik Petrosyan,[a] Annette-E. Surkus,[a] Stefan Lochbrunner,[b] and Jola Pospech*[a]

Herein we describe the synthesis and photophysical and electrochemical characterization of pyrimidopteridine-based photoredox catalysts. The pyrimidopteridines can be obtained from the corresponding *N*-oxides through photo-mediated oxygen atom transfer to a sacrificial acceptor molecule on gramscale. The presence of a triplet excited state was evidenced by means of transient absorption spectroscopy. Pyrimidopteridines are potent excited state oxidants with excited state reduction potentials exceeding +2.10 V vs. SCE in MeCN. The catalytic activity is illustrated in the photo-mediated oxidative annulation of 2-phenylbenzoic acid.

The development and investigation of photocatalytic systems is of paramount interest in organic chemistry.[1] The constant progress in this field fortifies the applicability of photoredox catalysis.[2] In addition to many transition metal-based photocatalysts, which undoubtedly have excellent and effective photo-physicochemical properties, the demand for metal-free photosensitizers is increasing.[3] Owing to the structural diversity of organic photoredox catalyst remarkably high oxidation potentials in the photo-excited state are accessible.[4] The comparatively low cost, low toxicity, and high abundance of organic photocatalysts, renders this substance class especially attractive.[5] In some instances, organic photoredox catalysts may imitate co-factors present in mammalian monooxygenases which reveal the possibility of developing bio-mimetic reactions.[6] The role of riboflavin has been intensively studied both in- and ex-vitro. The facile modulation of the redox reactivity and accessibility of multifaceted reactive intermediates render flavins essential co-factors in enzymes and synthetically versatile heterocyclic photoredox catalysts.[7] The group of Maki first synthesized structurally-related tetraalkylated pyrimidopteridine-*N*-oxides in 1986, revealing its potential as a stoichiometric oxygen atom transfer reagents in various photo-mediated reactions which led to biomimetic *N*-demethylation,[8] C–H oxygenation[9] and oxidative C–C bond cleavage.[10]

Recently, our group described the gram-scale synthesis of flavin related 1,3,7,9-tetraalkyl-2,4,6,8-tetraoxo-[5,4-g] pteridine 5-oxide (**PPTNO**) and characterization of its photophysical properties, qualifying these heteroarene-*N*-oxides as potent organic photoredox catalysts for seminal applications.[11] Thorough investigations concerning the photo-mediated decarboxylative Giese-type reaction and the photo-mediated hydroamination of stilbenes with primary amines, revealed the potency of the deoxygenated 1,3,7,9-tetraalkyl-2,4,6,8-tetraoxo-[5,4-g]pteridine (**PPT**) as catalytically active species.[12] Herein, we describe a convenient methodology for the deoxygenation of pyrimidopteridine-*N*-oxides (**PPTNO**) and the characterization of the photophysical and electrochemical characteristic of pyrimidopteridine (**PPT**) photoredox catalysts (Figure 1).

The deoxygenation of heteroarene-*N*-oxides can be accomplished through various methodologies.[13] The deoxygenation of pyrimidopteridine-*N*-oxides was previously accomplished

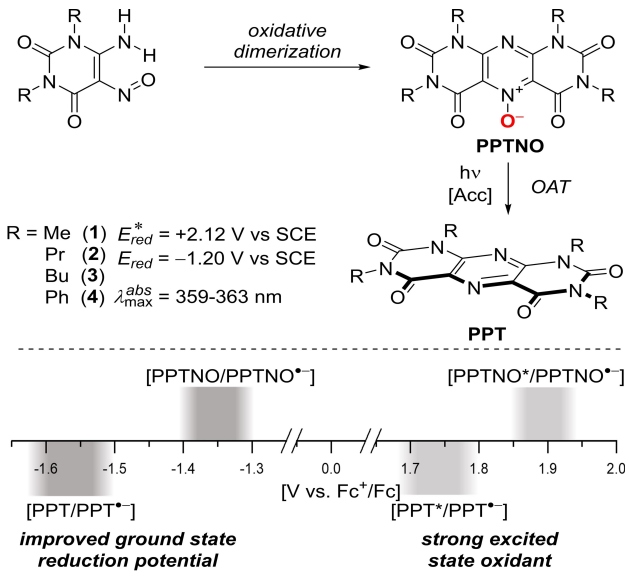

Figure 1. Synthesis and electrochemical properties of pyrimidopteridines (**1**–**4**).

[a] T. Taeufer,[+] Dr. A. Petrosyan, Dr. A.-E. Surkus, Dr. J. Pospech
Leibniz Institute for Catalysis
Albert-Einstein-Str. 29a, 18059 Rostock (Germany)
E-mail: Jola.Pospech@catalysis.de
[b] M. A. Argüello Cordero,[+] Prof. Dr. S. Lochbrunner
Institute for Physics and Department of Life, Light and Matter
Universität Rostock
18051 Rostock (Germany)
[+] These author contributed equally to this work.

Supporting information for this article is available on the WWW under https://doi.org/10.1002/cptc.202100159

Special Collection An invited contribution to the "GDCh and ChemPhotoChem: 5-Year Anniversary" Special Collection

through oxygen atom-transfer to anilines[8] and styrenes.[14] The most reliable methodology, in our hands, was the deoxygenation by photo-mediated oxygen atom transfer (OAT) to *trans*-stilbene. The corresponding pyrimidopteridines (**PPT**) were obtained in excellent yields (Scheme 1).

The *E*/*Z*-isomerization of stilbene is also promoted under these reaction conditions. Thus, an isomerization of the starting material and a mixture of *cis*- and *trans*-stilbene oxide was observed. Furthermore, oxidative cleavage of stilbene oxide resulted in the formation of benzaldehyde as a minor side-product.

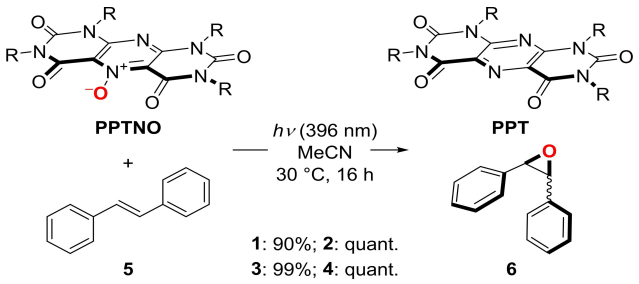

Scheme 1. Photochemical deoxygenation of pyrimidopteridines (**1**–**4**).

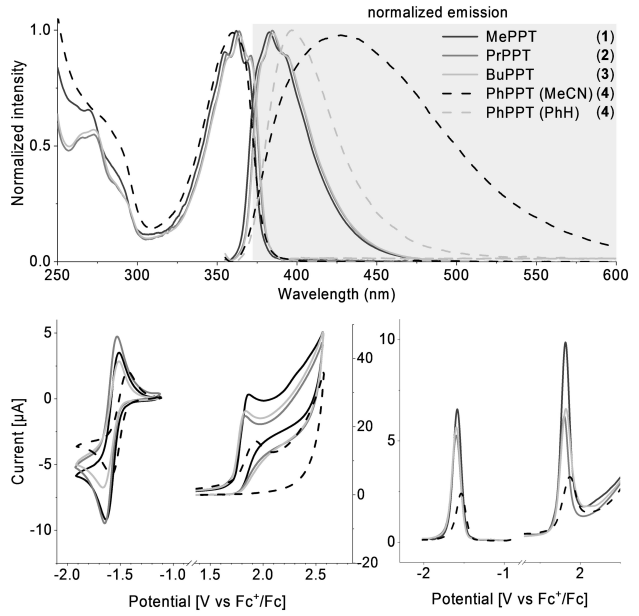

Figure 2. Normalized UV/Vis absorption and emission spectra (in MeCN, 20 μM) (top), cyclic voltammograms (CV, in MeCN, 1 mM, 40 mV s^{-1}) (bottom left) and differential pulse voltammograms (DPV in MeCN, 1 mM, 40 mV s^{-1}) (bottom right) of PPTs (**1**–**4**) against the Fc^+/Fc redox couple.

Next, the obtained pyrimidopteridines were examined concerning their photophysical properties (Figure 2). All **PPT** heteroarenes (**1**–**4**), here dissolved in MeCN, show an absorption maximum between 359 and 363 nm. The emission spectra of **1**–**3** exhibit a maximum between 383 and 385 nm. Heteroaromatic tetralkyl-substituted pyrimidopteridines (**1**–**3**) possess a very rigid molecular structure, resulting in a small Stokes shift of only 20 nm (0.19 eV). Single crystal X-ray crystal structures for compounds **1**–**4** are reported in the Supporting Information.[19]

The emission spectra of **1**, **2** and **3** exhibit close to mirror-image symmetry with respect to the absorption and the quantum yields are between 59 and 66%. In contrast, the emission spectrum of phenyl-bearing **4** has a broad shape with a maximum at 427 nm, indicative of an enhanced charge-transfer character in the excited state in the presence of aryl substituents on the pyrimidopteridine core. To check this notion the emission of **4** was also recorded in benzene which exhibits a much lower relative permittivity of 2.3 than MeCN with a permittivity of 38. The Stokes shift in benzene is indeed quite small, see Figure 2, demonstrating that the excited state has a large dipole moment and strong charge-transfer character. This results also in a decreased quantum yield of 10%. The fluorescence lifetimes of all compounds were determined to be between 2.1 and 2.9 ns. The $E_{0,0}$ values listed in Table 1 correspond to the energy at the intersection of the absorption and emission spectra in MeCN and are between 372–376 nm (3.30–3.33 eV) for PPT **1**–**4**. Since structurally related flavins exhibit rather high triplet yields[15] we performed transient absorption (TA) measurements with an ultrafast pump-probe setup to check for the appearance of long lived dark states.

Figures 3a and 3b show TA spectra of **2** and **4** in MeCN after optical excitation at 360 nm. For **2** ground state bleach (GSB) and stimulated emission (SE) are observed in the near UV as well as an excited state absorption (ESA) band at around 490 nm. The features show some changes within the experimentally accessible time window of 2 ns but a large fraction of the TA persists for longer times. The dynamics was analysed by a multiexponential global fit, see Figure 3c. To include the depopulation of the S_1 state one decay time was set to the fluorescence lifetime of 2.8 ns and to account for a long-lived dark state another decay time was set to

Table 1. Photophysical and electrochemical properties of PPT photoredox catalysts.

Compound	λ^{abs}_{max} [nm]	λ^{em}_{max} [nm]	Φ_f [%]	τ [ns]	$E_{0,0}$ [V] [c]	$E^{red}_{1/2}$ [V vs Fc^+/Fc][a]	$E^{ox}_{1/2}$ [V vs Fc^+/Fc][a]	$E^{red}_{1/2}$ [V vs SCE] [b]	$E^{ox}_{1/2}$ [V vs SCE] [b]	E_{red}* [V vs Fc^+/Fc] [d]	E_{ox}* [V vs Fc^+/Fc] [d]	E_{red}* [V vs SCE] [d]	E_{ox}* [d]
MePPT (**1**)	361	383	66	2.89	+3.33	−1.58	+1.82	−1.20	+2.20	+1.75	−1.51	+2.13	−1.13
PrPPT (**2**)	363	385	59	2.82	+3.31	−1.59	+1.80	−1.21	+2.18	+1.72	−1.51	+2.10	−1.13
BuPPT (**3**)	363	385	63	2.90	+3.31	−1.59	+1.82	−1.21	+2.20	+1.72	−1.49	+2.10	−1.11
PhPPT (**4**)	359	427	10	2.14	+3.30	−1.54	+1.87	−1.16	+2.25	+1.76	−1.43	+2.14	−1.05

[a] Potentials were measured using cyclic voltammetry (CV) and differential pulse voltammetry (DPV) relative to Fc^+/Fc. [b] Referenced to SCE by adding 0.38 V to the value relative to Fc^+/Fc.[15] [c] $E_{0,0}$ values corresponding to the energy at the intersection of the excitation and emission spectra. [d] Calculated by $E_{red}^* = E_{0,0} + E^{red}_{DPV}$ and $E_{ox}^* = E^{ox}_{DPV} - E_{0,0}$.

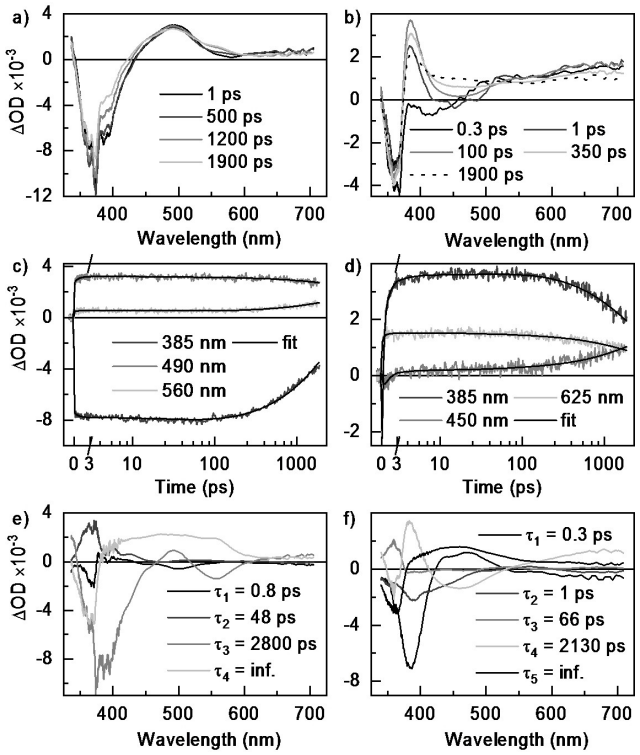

Figure 3. TA spectra of **2** (left) and **4** (right) after excitation at 360 nm at the given delay times (a and b), kinetics at selected probe wavelengths and related time traces of a global multiexponential fit (c and d), and DAS labelled by the corresponding decay times (e and f). Both substances were measured in MeCN using kuvettes with a thickness of 1 mm. The optical density was approximately 0.6 for each solution at the excitation wavelength.

infinity. The decay associated spectrum (DAS) of the 2.8 ns component reflects, as expected, the disappearance of the SE around 390 nm, a partial recovery of the GSB and the rise of an ESA band at 560 nm, see Figure 3e. The long-lived component exhibits a large GSB contribution, too, and a broad ESA whose red wing resembles the ESA formed during the S_1 decay. The long lived state is most probably the triplet state since it exhibits no emission and for flavins TA experiments revealed similar features due to population of triplet states.[15] There, the ESA is located more to the red but this is in line with the lower S_1 energy of flavins compared to the **PPT**s. Since the GSB contributions of the 2.8 ns and the long-lived component are of similar strength we estimate that about half of the molecules in the S_1 state undergo intersystem crossing while the rest decays radiatively back to the ground state. The fit also contains two faster components whose DAS have a significant amplitude only around the excitation wavelength of 360 nm. The fastest one with a time constant of 0.8 ps is assigned to vibrational redistribution processes and the other one with a decay time of 48 ps to a reminiscence of orientational relaxation. The latter assignment is based on additional measurements with parallel and perpendicular polarizations of pump and probe in which this component is very strong and exhibits opposite signs. In the here presented measurements the polarizations were set to the magic angle in order to suppress signatures caused by orientational relaxation. The TA spectra of **4**, shown in Figure 3b and corresponding fits and DASs in Figures 3d and 3f, exhibit on longer time scales dynamics similar to **2** but at shorter times additional features due to electron transfer. The fastest component with a time constant of 0.3 ps describes the disappearance of the emission from the optically populated S_1 state and the rise of the charge transfer fluorescence at 450 nm. The 0.3 ps time can therefore be identified with the duration of the electron transfer step. The 1 ps component reflects a further red shift of the charge transfer fluorescence which might be caused by relaxation of the solvent shell. The small 66 ps contribution is again a reminiscence of orientational relaxation. The component with a time constant of 2130 ps describes the decay of the charge transfer fluorescence and a partial recovery of the GSB while the long-lived component consists of the remaining GSB and a broad ESA. The latter is again attributed to the triplet state which is populated from the electron transfer state by a rather large fraction of the molecules.

The redox properties in the ground state ($E^{red}_{1/2}$ and $E^{ox}_{1/2}$) were determined by cyclic voltammetry (CV) and differential pulse voltammetry (DPV) against the ferrocene redox couple Fc^+/Fc (Figure 2). In addition, the measured values are reported with respect to the reference system of a saturated calomel electrode (SCE).[16] All compounds show an irreversible anodic oxidation above +2.20 V vs SCE and a reversible reduction at approximately −1.20 V vs SCE in MeCN. The excited state potentials of the pyrimidopteridines **PPT**s were determined using the optical and electrochemical data. The observed heterocycles are excellent excited state oxidants with excited state reduction potentials E_{red}^* above +2.10 V vs SCE in MeCN. The excited state reduction potentials are systematically lower than those of the corresponding *N*-oxides by approximately 0.15 V, however by utilizing the deoxygenated heteroarene a disturbing initial oxygen atom transfer can be circumvented in a photocatalytic reaction.

Mechanistically, the deoxygenation of pyrimidopteridine-*N*-oxides proceed via excitation of the *N*-oxide ($E_{red}^* > 2.26$ V vs SCE in MeCN)[17] and subsequent single electron oxidation of stilbene ($E^{ox}_{1/2} = 1.56$ V vs SCE in MeCN).[12b] The nucleophilic attack of the *N*-oxide oxygen to the radical cation of stilbene is followed by homolytic N–O bond cleavage and radical recombination to form stilbene oxide (**6**) and plain pyrimidopteridine (Scheme 2).

The catalytic activity of the deoxygenated pyrimidopteridines **PPT** was tested in the photo-mediated oxidative annulation of 2-phenylbenzoic acid (**7**), according to a protocol previously reported by Gilmour and co-workers.[18] The desired cyclization product 6*H*-benzo[*c*]chromen-6-one (**8**) was obtained in 66–86% isolated yield under unoptimized reaction conditions (Scheme 3). The yields correlate with the excited state reduction potentials of the respective **PPT**s.

In summary, we reported the synthesis, photo- and electrochemical characterization and application of pyrimidopteridine based photoredox catalysts. The described

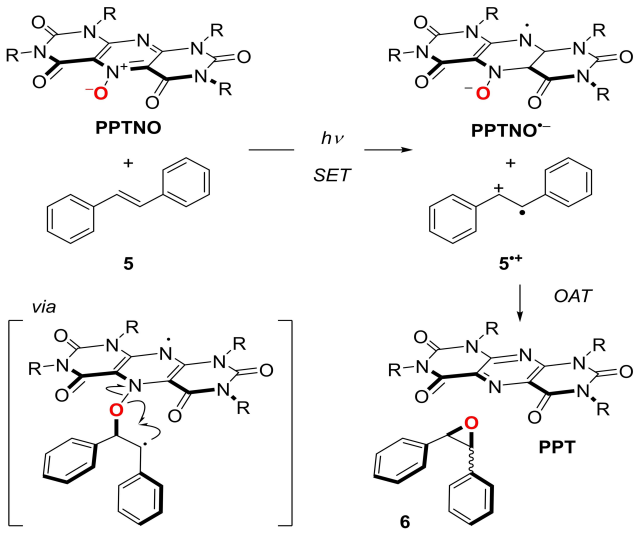

Scheme 2. Mechanistic proposal for the photomediated deoxygenation of pyrimidopteridine-*N*-oxide (PPTNO) in the presence of stilbene.

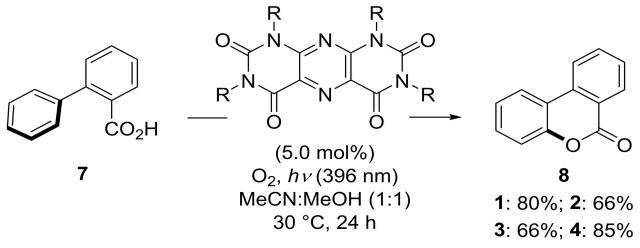

Scheme 3. Oxidative annulation of 2-phenyl benzoic acid (**7**).

heteroarene based photosensitizers are potent photooxidants with excited state reduction potentials exceeding +2.10 V vs SCE in MeCN. **1**, **2**, and **3** exhibit in MeCN a fluorescence quantum yield of about 60% and a S_1 lifetime of 2.8–2.9 ns while in **4** the quantum yield is decreased to 10% and the lifetime to 2.1 ns. TA measurements indicate that a large fraction of optically excited molecules experience intersystem crossing. In **4**, in addition, a fast electron transfer within 0.3 ps after the excitation occurs. We have demonstrated that the corresponding pyrimidopteridine-*N*-oxides serve as photoredox-active pre-catalyst to pyrimidopteridines which is activated by photo-mediated oxygen atom transfer (OAT) to an appropriate oxygen atom acceptor. The synthesis of four pyrimidopteridines through photo-mediated deoxygenation in the presence of stilbene for the gram-scale synthesis of pyrimidopteridines and a plausible mechanistic pathway were described. The catalytic activity of pyrimidopteridine-based heterocycles is demonstrated in the photo-mediated oxidative annulation of 2-phenylbenzoic acid.

Acknowledgements

This work was funded by the Deutsche Forschungsgemeinschaft (DFG, German Research Foundation) 401007518 and by the European Social Fund (ESF/14-BM-A55-0049/16). We thank Dr. Anke Spannenberg (LIKAT) and Dr. Alexander Villinger (Rostock University) for crystallographic measurements. Moreover, we would like to express our gratitude to the LIKAT for excellent support. Open Access funding enabled and organized by Projekt DEAL.

Conflict of Interest

The authors declare no conflict of interest.

Keywords: organic photoredox catalysis · pyrimidopteridines · deoxygenation · *N*-oxides · heteroarenes

[1] a) B. König, *Eur. J. Org. Chem.* **2017**, *2017*, 1979–1981; b) G. E. M. Crisenza, P. Melchiorre, *Nat. Commun.* **2020**, *11*, 803.
[2] a) T. P. Nicholls, D. Leonori, A. C. Bissember, *Nat. Prod. Rep.* **2016**, *33*, 1248–1254; b) J. J. Douglas, M. J. Sevrin, C. R. J. Stephenson, *Org. Process Res. Dev.* **2016**, *20*, 1134–1147; c) R. C. McAtee, E. J. McClain, C. R. J. Stephenson, *Trends Chem.* **2019**, *1*, 111–125; d) D. Petzold, M. Giedyk, A. Chatterjee, B. König, *Eur. J. Org. Chem.* **2020**, *2020*, 1193–1244.
[3] a) E. Speckmeier, T. G. Fischer, K. Zeitler, *J. Am. Chem. Soc.* **2018**, *140*, 15353–15365; b) Y. Lee, M. S. Kwon, *Eur. J. Org. Chem.* **2020**, *2020*, 6028–6043.
[4] a) A. Joshi-Pangu, F. Lévesque, H. G. Roth, S. F. Oliver, L.-C. Campeau, D. Nicewicz, D. A. DiRocco, *J. Org. Chem.* **2016**, *81*, 7244–7249; b) H. Huang, Z. M. Strater, M. Rauch, J. Shee, T. J. Sisto, C. Nuckolls, T. H. Lambert, *Angew. Chem. Int. Ed.* **2019**, *58*, 13318–13322; *Angew. Chem.* **2019**, *131*, 13452–13456; c) S. Wu, J. Žurauskas, M. Domański, P. S. Hitzfeld, V. Butera, D. J. Scott, J. Rehbein, A. Kumar, E. Thyrhaug, J. Hauer, J. P. Barham, *Org. Chem. Front.* **2021**, *8*, 1132–1142; d) P. Natarajan, B. König, *Eur. J. Org. Chem.* **2021**, *2021*, 2145–2161.
[5] N. A. Romero, D. A. Nicewicz, *Chem. Rev.* **2016**, *116*, 10075–10166.
[6] a) J. B. Metternich, R. Gilmour, *J. Am. Chem. Soc.* **2015**, *137*, 11254–11257; b) T. Hering, B. Mühldorf, R. Wolf, B. König, *Angew. Chem. Int. Ed.* **2016**, *55*, 5342–5345; *Angew. Chem.* **2016**, *128*, 5428–5431; c) V. Srivastava, P. K. Singh, A. Srivastava, P. P. Singh, *RSC Adv.* **2021**, *11*, 14251–14259.
[7] a) R. Teufel, V. Agarwal, B. S. Moore, *Curr. Opin. Chem. Biol.* **2016**, *31*, 31–39; b) S. Adak, T. P. Begley, *Arch. Biochem. Biophys.* **2017**, *632*, 4–10; c) E. Romero, J. R. Gómez Castellanos, G. Gadda, M. W. Fraaije, A. Mattevi, *Chem. Rev.* **2018**, *118*, 1742–1769.
[8] M. Sako, K. Shimada, K. Hirota, Y. Maki, *J. Am. Chem. Soc.* **1986**, *108*, 6039–6041.
[9] a) M. Sako, S. Ohara, K. Hirota, Y. Maki, *J. Chem. Soc. Perkin Trans. 1* **1990**, *12*, 3339–3344; b) M. Sako, K. Hirota, Y. Maki, *Chem. Pharm. Bull.* **1990**, *38*, 2069–2071; c) M. Sako, S. Ohara, K. Shimada, K. Hirota, Y. Maki, *J. Chem. Soc. Perkin Trans. 1* **1990**, *4*, 863–868.
[10] a) M. Sako, K. Shimada, K. Hirota, Y. Maki, *Tetrahedron Lett.* **1986**, *27*, 3877–3880; b) Y. Maki, M. Sako, I. Oyabu, T. Murase, Y. Kitade, K. Hirota, *J. Chem. Soc. Chem. Commun.* **1989**, 1780–1782; c) Y. Maki, I. Oyabu, S. Ohara, M. Sako, Y. Kitade, K. Hirota, *Chem. Pharm. Bull.* **1989**, *37*, 3239–3242.
[11] R. Hauptmann, A. Petrosyan, F. Fennel, M. A. Argüello Cordero, A.-E. Surkus, J. Pospech, *Chem. Eur. J.* **2019**, *25*, 4325–4329.
[12] a) F. El-Hage, C. Schöll, J. Pospech, *J. Org. Chem.* **2020**, *85*, 13853–13867; b) T. Taeufer, R. Hauptmann, F. El-Hage, T. S. Mayer, H. Jiao, J. Rabeah, J. Pospech, *ACS Catal.* **2021**, *11*, 4862–4869.
[13] a) R. Balicki, M. Cybulski, G. Maciejewski, *Synth. Commun.* **2003**, *33*, 4137–4141; b) H. Sterckx, C. Sambiagio, V. Médran-Navarrete, B. U. W. Maes, *Adv. Synth. Catal.* **2017**, *359*, 3226–3236; c) S. P. Zucker, F. Wossidlo, M. Weber, D. Lentz, C. C. Tzschucke, *J. Org. Chem.* **2017**, *82*,

5616–5635; d) K. D. Kim, J. H. Lee, *Org. Lett.* **2018**, *20*, 7712–7716; e) Y. Fukazawa, A. E. Rubtsov, A. V. Malkov, *Eur. J. Org. Chem.* **2020**, *2020*, 3317–3319; f) M. Fukui, A. Tanaka, H. Kominami, *Ind. Eng. Chem. Res.* **2020**, *59*, 11412–11418; g) M. O. Konev, L. Cardinale, A. Jacobi von Wangelin, *Org. Lett.* **2020**, *22*, 1316–1320.
[14] M. Sako, S. Ohara, K. Hirota, Y. Maki, *Tetrahedron* **1990**, *46*, 4171–4178.
[15] J. T. M. Kennis, S. Crosson, M. Gauden, I. H. M. van Stokkum, K. Moffat, R. van Grondelle, *Biochemistry* **2003**, *42*, 3385–3392.
[16] V. V. Pavlishchuk, A. W. Addison, *Inorg. Chim. Acta* **2000**, *298*, 97–102.
[17] H. G. Roth, N. A. Romero, D. A. Nicewicz, *Synlett* **2016**, *27*, 714–723.
[18] a) J. B. Metternich, R. Gilmour, *J. Am. Chem. Soc.* **2016**, *138*, 1040–1045; b) T. Morack, J. B. Metternich, R. Gilmour, *Org. Lett.* **2018**, *20*, 1316–1319.
[19] Deposition Number 2080119 2080120 2080121 2081870 (for compounds **1**–**4**) contain the supplementary crystallographic data for this paper. These data are provided free of charge by the joint Cambridge Crystallographic Data Centre and Fachinformationszentrum Karlsruhe Access Structures service www.ccdc.cam.ac.uk/structures.

Manuscript received: July 30, 2021
Revised manuscript received: August 17, 2021
Accepted manuscript online: August 26, 2021
Version of record online: September 12, 2021